

CALLISTO: NEW INSIGHTS FROM *GALILEO* DISK-RESOLVED UV MEASUREMENTS

AMANDA R. HENDRIX

Jet Propulsion Laboratory/California Institute of Technology, 4800 Oak Grove Drive,
Pasadena, CA 91109; arh@jpl.nasa.gov

AND

ROBERT E. JOHNSON

University of Virginia, Thornton Hall B102, P.O. Box 400238, Charlottesville, VA 22904

Received 2008 April 4; accepted 2008 June 10

ABSTRACT

The entire set of observations from the *Galileo* Ultraviolet Spectrometer (UVS) is analyzed to look for spectral trends across the surface of Callisto, and to probe the spectral shapes in the near-UV. At low resolution, the leading hemisphere is slightly redder than the trailing hemisphere at $\lambda > 280$ nm; this has been interpreted by past researchers to indicate the presence of SO₂ on the leading hemisphere. Here we point out that such an “absorption feature” can be induced when ratioing hemispherical spectra. High-resolution observations are used to detect the presence of an absorption band at high southern latitudes, interpreted to be due to some organic species that is weathered away (carbonized) at lower latitudes. The presence of CO₂ in the surface and in the atmosphere of Callisto and the dark nature of the surface suggest that carbon-based species are present across the surface associated with either endogenic or delivered organics. These organics experience chemical modification by UV radiation and are mixed into the regolith by meteoritic bombardment.

Subject headings: planets and satellites: general — planets and satellites: individual (Callisto) — ultraviolet: solar system

1. INTRODUCTION

Callisto is a notable end-member among the Galilean satellites, being darker and more heavily cratered than Ganymede and Europa, and playing a significant role in the understanding of icy moon evolution (Moore et al. 2004). Although its radiation environment is not negligible, Callisto is farther from Jupiter and evidently outside the region of intense plasma bombardment (Johnson et al. 2004). Callisto thus presents a useful case for comparisons with the other satellites, whose histories appear to include more geologic activity and whose surfaces may be significantly affected by energetic particle bombardment. In the case of Europa, the surface is highly influenced by the energetic particles trapped in Jupiter’s magnetosphere; at Ganymede such bombardment occurs primarily at its poles, with much of the low-latitude region partially shielded from energetic particles by Ganymede’s magnetic field.

We present results from an investigation of the *Galileo* Ultraviolet Spectrometer (UVS) data of Callisto in the 210–320 nm wavelength range. The nature of Callisto’s dark, red UV reflectance spectra is investigated in order to understand the composition and space weathering of the surface. We explore absorption feature variations across the surface and their possible relationship with exogenic processing and implanted and/or endogenic materials. We begin with a brief review of the surface composition and surface processes of importance at Callisto.

2. BACKGROUND

Ground-based and *Galileo* VNIR data sets (e.g., Pilcher et al. 1972; McCord et al. 1997) have shown that Callisto’s surface composition consists primarily of water ice plus at least one non-water ice component. Candidates for the non-water ice components include phyllosilicates (Roush et al. 1990; Calvin & Clark 1991), and small features due to organics were suggested to be present at

NIR wavelengths (McCord et al. 1997). Carbon dioxide is present at the surface, particularly in dark regions, possibly adsorbed or trapped in grains of non-ice material, based on the presence of an absorption feature at 4.25 μm (Hibbitts et al. 2000), and this surface CO₂ feature is distinct from the absorption expected from crystalline CO₂.

The surface weathering processes thought to contribute to Callisto’s spectral reflectance are sublimation, micrometeoroid bombardment, radiation-induced chemistry and sputtering, and implantation of sulfur ions or neutrals from Io. Presumably as a result of these effects, Callisto displays a hemispherical dichotomy that is opposite that of Europa and Ganymede. Although its albedo is low relative to those bodies, its trailing hemisphere has a slightly higher albedo than its leading hemisphere (Stebbins & Jacobsen 1928); however, at 0° solar phase angle, the leading hemisphere is brighter than the trailing hemisphere. This has been ascribed to preferential contamination of the leading hemisphere by micrometeoroid bombardment (Buratti 1991), consistent with the suggestion that Callisto’s trailing hemisphere has larger grains than the leading hemisphere (Calvin & Clark 1993). Callisto’s albedo dichotomy is present both at visible wavelengths and in the near-UV (Nelson et al. 1987; Hendrix et al. 2005).

Iogenic material reaching Callisto as a neutral wind was proposed to explain an absorption feature detected on Callisto’s leading Jovian-facing hemisphere. The UV feature seen by Lane & Domingue (1997) and Noll et al. (1997) appeared to resemble the 280 nm absorption feature seen on Europa, primarily on the trailing hemisphere, which is likely due to SO bonds (Lane et al. 1981).

The fact that Europa, Ganymede, and Callisto all orbit Jupiter within the powerful Jovian magnetosphere can have a profound effect on their surfaces. The Galilean satellites are each phase-locked with Jupiter, so that one hemisphere (the Jovian hemisphere, centered on 0° longitude) is always facing Jupiter. The hemisphere

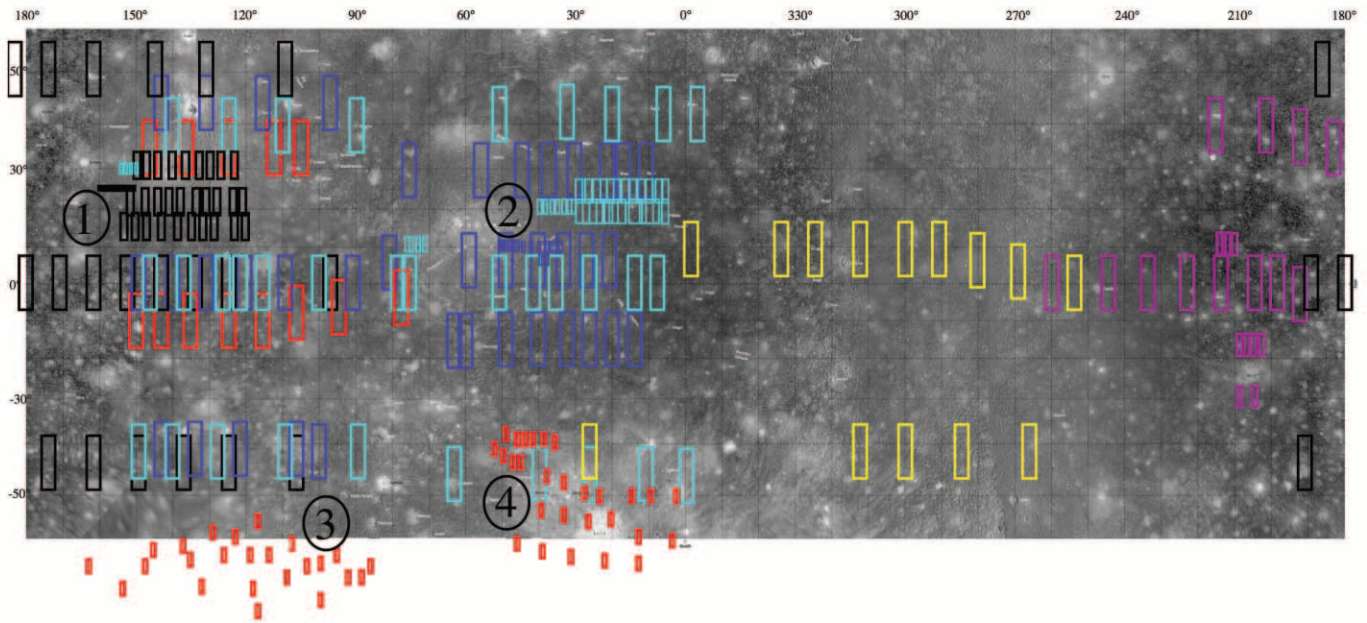


FIG. 1.—Map of Callisto showing observational coverage by the *Galileo* UVS. Each box indicates the IFOV (instantaneous field of view) size during a particular observation sequence. Numbered regions are discussed in the text. Colors represent fly-bys (black: C3; red: G6; white: G7; blue: C9; cyan: C10; yellow: E14; purple: C20). Larger FOVs correspond to low-resolution (or global-scale) observations, while smaller FOVs correspond to high-resolution observations.

leading in the direction of orbital motion (leading hemisphere) is centered on 90° west longitude, while the trailing hemisphere is centered on 270° west. Because Jupiter’s magnetosphere corotates at a rate faster than the orbital speed of these moons, the satellites’ trailing hemispheres are preferentially affected by magnetospheric particle bombardment (cold ions and energetic electrons). Due to the differences in flux with distance from Jupiter among the icy satellites, charged particle bombardment has the largest effect on Europa, which, being the closest to Jupiter, experiences the highest flux of particles, and the smallest effect on Callisto, with the most distant orbit and the lowest particle flux. In addition, due to its distance from Jupiter, Callisto is not always fully immersed in the plasma sheet, but travels in and out as a result of the tilt of the axis of Jupiter’s magnetic field (Cooper et al. 2001). Callisto also has a more robust protective atmosphere as discussed below. On Europa, a result of the charged particle bombardment is a relatively dark trailing hemisphere. Although magnetospheric ion bombardment (and its associated sputtering, implantation, grain size alteration, and chemical modification) is a much weaker alteration process at Callisto’s orbit, very energetic electrons and ions can have access to the surface and have been considered in interpreting the CO_2 pattern on Callisto’s trailing hemisphere (Hibbitts et al. 2000). Also, molecular oxygen has been detected on the trailing hemisphere of Callisto (Spencer & Calvin 2002), although it is unclear whether the O_2 is a result of particle radiation. The O_2 feature also appears on Europa’s leading and trailing hemispheres, and on Ganymede’s trailing hemisphere at low latitudes, which may be partially protected from radiolysis by Ganymede’s intrinsic magnetic field.

Since the energy flux of UV photons (those energetic enough to dissociate water ice) is higher at Callisto than the energy flux of energetic particles, photolysis can dominate the radiation chemistry (Johnson et al. 2004). Furthermore, being darker, the surface of Callisto is warm compared to Europa and Ganymede; Callisto’s subsolar temperature is ~ 168 K compared with ~ 156 K at Ganymede and ~ 132 K at Europa. Since the chemistry produced by radiolysis or photolysis can be a strong function of temperature,

chemical differences are expected among the satellites. The temperature difference also means that sublimation-induced resurfacing and cold trapping on shaded surfaces is faster at Callisto.

Callisto may have a much thicker atmosphere than either Europa or Ganymede (Liang et al. 2005). The CO_2 component of the atmosphere was first detected by *Galileo* NIMS (Carlson 1999), but modeling suggests a more robust atmosphere (Strobel et al. 2002). Consistent with this, the ionosphere (Kliore et al. 2002) is also more substantial and appears to be present only when the trailing hemisphere is illuminated by the Sun. Since no emission features were detected at FUV wavelengths that would be a result of electron excitation and dissociation of CO_2 (Strobel et al. 2002), it was suggested that the interaction between the ionosphere and Jupiter’s magnetosphere effectively reduces the electron impact induced emission rate. A relatively thick atmosphere also protects the surface from a significant fraction of the charged particle flux.

3. OBSERVATIONS AND ANALYSIS

The *Galileo* UVS was built at the University of Colorado’s Laboratory for Atmospheric and Space Physics and is described by Hord et al. (1992). The observations discussed in this paper were performed using the F-channel of the UVS, which covers the 161.6–321.3 nm wavelength range. The calibration is described by Hendrix (1996). The observations were performed in “full-scan” mode, where the grating was stepped over the 528 channels covering the wavelength range in 4.33 s, with 0.006 s integration time at each channel. The UVS instantaneous field of view (IFOV) was $0.1^\circ \times 0.4^\circ$, and measurements are generally classified as low-resolution (or global-resolution) or high-resolution, made from distances of $\sim 200,000$ or $\sim 20,000$ km, respectively. During the *Galileo* mission (1996–2000), the UVS performed observations covering much of the surface of Callisto, focusing on the leading hemisphere. A map indicating the coverage of Callisto obtained by the *Galileo* UVS is shown in Figure 1. Primary targets were the regions surrounding the Asgard impact basin

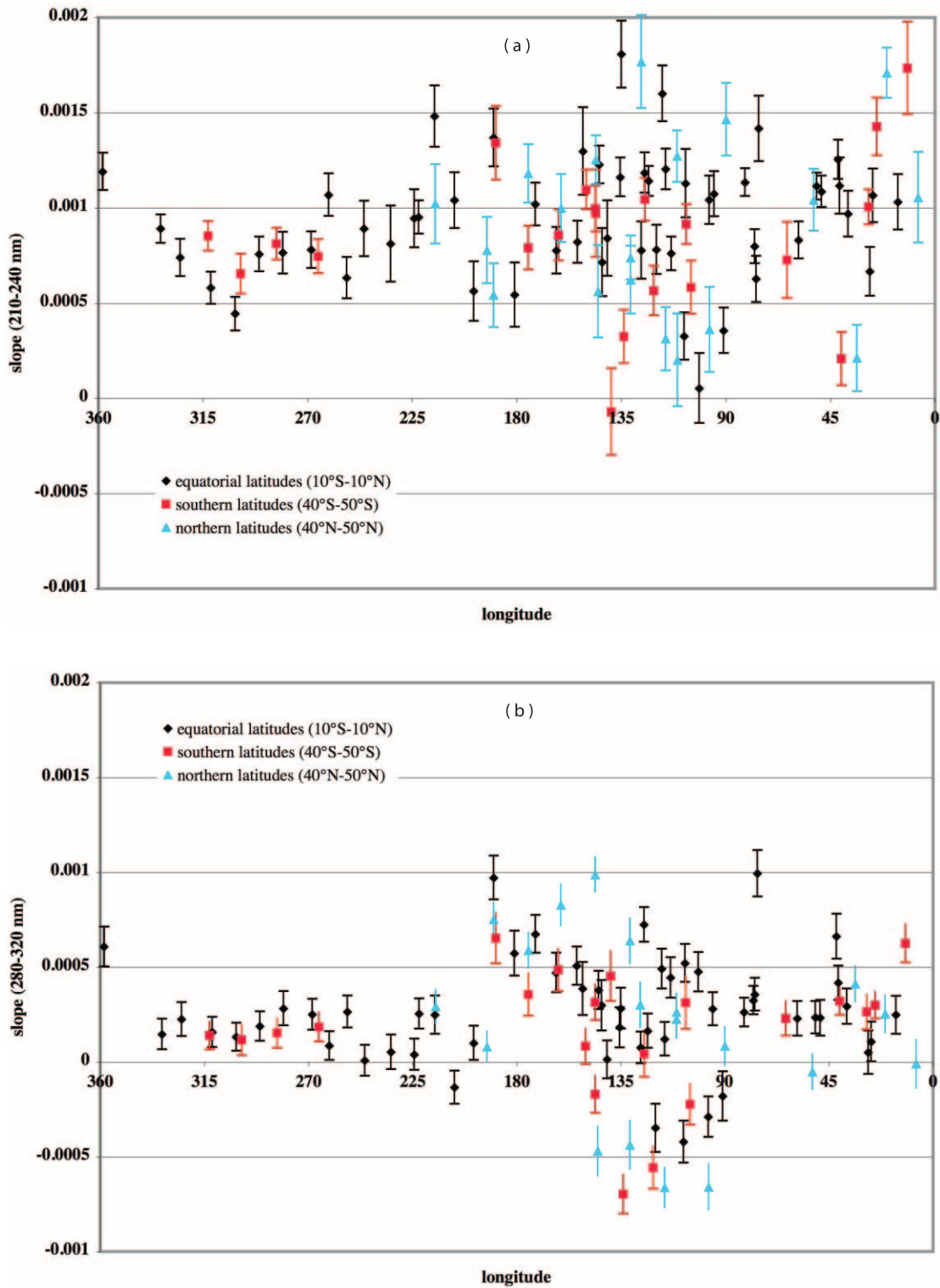


FIG. 2.—Global-scale observation spectral slopes for (a) 220–240 nm and (b) 280–320 nm vs. longitude. Across the surface, reflectance spectra are red in slope in the 220–240 nm region and relatively flat in the 280–320 nm region. Slopes are in units of reflectance per Å. Error bars represent the 1σ uncertainty on the computed slopes.

on the anti-Jovian/leading quadrant (central latitude/longitude of approximately 30° north/ 140° west, Fig. 1, region 1), and the Valhalla impact basin on the jovian/leading quadrant (central latitude/longitude of approximately 5° north/ 55° west, Fig. 1, region 2). Observations of the south polar region were also made (Fig. 1, regions 3 and 4).

For every observation in the UVS database, we applied the same reduction and analysis technique, as follows. Each spec-

trum, a total of 14 grating scans (60.67 s total integration), was converted to a reflectance spectrum by subtracting background, applying calibration, and dividing by the solar spectrum. The solar spectrum was measured by the Solar-Stellar Irradiance Comparison Experiment (SOLSTICE) (Rottman et al. 1993) and was double boxcar-smoothed to match the UVS resolution. The background signal primarily includes system radiation signal and is wavelength-independent. The background level is determined by

averaging the signal at the lowest wavelengths, where reflected sunlight does not contribute to the measured signal.

The *Galileo* UVS instrument was calibrated in terms of what would be observed from an extended source, in units of $10^6/4\pi \text{ cm}^{-2} \text{ s}^{-1} \text{ sr}^{-1} \text{ \AA}^{-1}$. The calibrated measurements are brightness = $4\pi I$. Because the SOLSTICE-measured solar spectrum is πF , the reflectance is given as $r = I/4F$, where the solar spectrum is corrected for the Sun-Jupiter distance.

4. RESULTS

We have investigated all Callisto reflectance spectra of suitable quality and explore the overall spectral shape in the near-UV. All of the reflectance spectra increase in brightness with wavelength over the 200–320 nm range (i.e., they are spectrally red). There is often a slope change at ~ 280 nm (also seen in earlier Earth-based observations), so we have taken the approach of fitting each spectrum with straight lines to determine the slope in the 280–320 and 220–240 nm wavelength ranges. In determining slopes, we remove brightness variations due to phase angle variations by first normalizing each spectrum to unity at 255 nm. We use only spectra of adequate signal-to-noise ratio ($S/N > 5$ at 280 nm). We utilize these spectral slopes, from both low- and high-resolution observations, to look for trends in spectral shape across the surface of Callisto.

4.1. Spectral Trends—Global Resolution

We first address the low-resolution, or global-scale, observations. Spectral slopes are shown in Figure 2. Nearly all spectra have a slight red slope at $\lambda < 240$ nm and a flat-to red slope at $\lambda > 280$ nm. We do not detect any significant relationships between spectral shape and latitude at this resolution; similarly, the spectral shape does not vary considerably with longitude. The trailing hemisphere (centered on 270° west) appears to be fairly uniformly spectrally flat at $\lambda > 280$ nm, but the trailing hemisphere data set is sparser than that of the leading hemisphere (centered on 90° west). Thus, at low resolution we do not detect any noteworthy spectral changes at the global scale corresponding to the Asgard or Valhalla impact basins. Average reflectance spectra from the trailing and leading hemispheres are shown in Figure 3a, to demonstrate the spectral shapes. Overall, there is a small difference between the central leading and central trailing hemisphere spectra, where the leading hemisphere is slightly redder at $\lambda > 280$ nm. Past researchers (Lane & Domingue 1997; Noll et al. 1997) attributed this spectral difference to the presence of SO_2 on the leading hemisphere, with a broad absorption feature centered at 280 nm as indicated by the ratio in Figure 3b; this is discussed more below.

4.2. A High-Latitude Absorption Feature— A Detection of Organics?

We perform the same analysis on the high-resolution observations as on the global-resolution observations, namely, fitting the spectral regions 220–240 and 280–320 nm with straight lines to look for trends across the surface in spectral shape. Focusing on the high-resolution observations, distinct trends in spectral shape are seen across the surface, as seen in Figure 4.

Looking first at the Valhalla and Asgard regions in Figure 4, we see that the Asgard spectra (primarily the black data points centered on $\sim 140^\circ$ west) are largely redder at $\lambda > 280$ nm than the Valhalla spectra (primarily the blue data points centered on $\sim 35^\circ$ west); i.e., the Asgard spectra have steeper slopes at $\lambda > 280$ nm. Meanwhile, at high southern latitudes (G8 south pole in

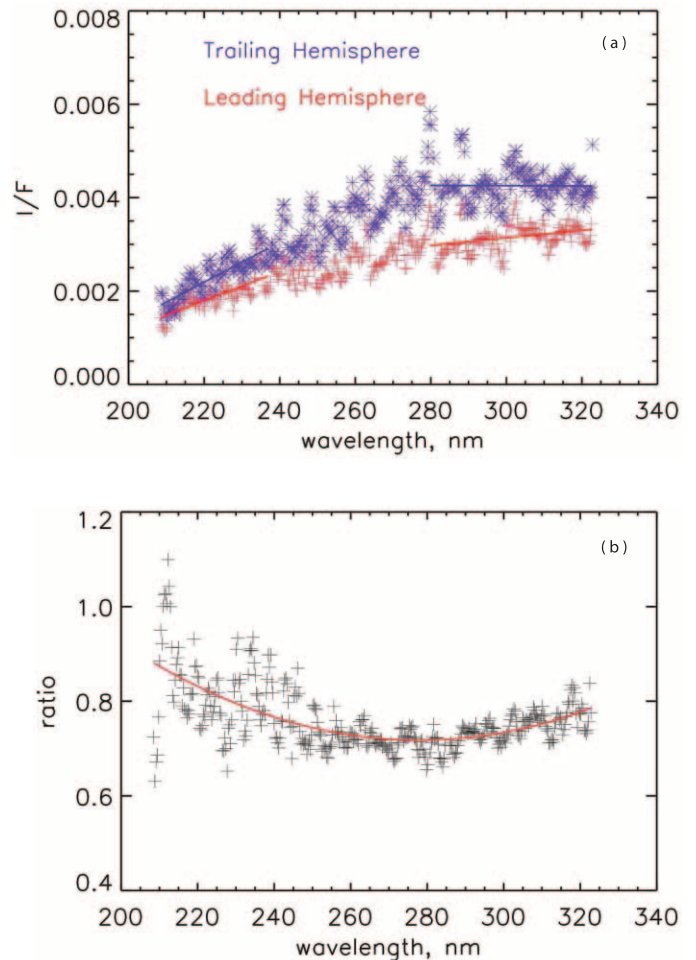


FIG. 3.—(a) Average reflectance spectra of the leading and trailing hemispheres, both at $\sim 70^\circ$ phase angle (equatorial latitudes, using global-resolution observations). (b) The ratio of the leading hemisphere to the trailing hemisphere exhibits a broad, weak absorption band; the red line is a polynomial fit to the ratio, to help guide the eye. The leading hemisphere spectrum is an average of spectra from the G8 GLOBAL observation, longitudes 77° – 135° west; the trailing hemisphere spectrum is an average of spectra from the C20 GLOBAL observation, longitudes 224° – 261° west.

Fig. 4; regions 3 and 4 in Fig. 1), the spectrum is the same as the other two below ~ 280 nm but is spectrally blue at $\lambda > 280$ nm as seen in Figure 5, where an average Valhalla-region spectrum, an average Asgard-region spectrum, and an average south polar region spectrum are normalized and compared. The consistency in the wavelength dependence in the three spectra is striking below ~ 280 nm. However, it is seen that at $\lambda > 280$ nm there is a spectral “rollover” of the south polar region suggestive of the shoulder of an absorption feature with a band center above 320 nm. The UV rollover feature was not identified in previous Earth-based disk-integrated observations of Callisto (Nelson et al. 1987; Lane & Domingue 1997; Noll et al. 1997). This is likely because the feature is predominantly at high latitudes and does not contribute significantly when viewing from Earth, although some spectra in Figures 2–4 in Lane & Domingue (1997) are not inconsistent with such a feature being present. We also note that an absorption feature at this wavelength appears to be unique to Callisto, as it was not identified in *Galileo* UVS spectra of Europa (Hendrix et al. 1998) or Ganymede (Hendrix et al. 1999). The disk-averaged ozone feature at Ganymede appeared to have a shoulder suggested to be due to a $-\text{CH}_2\text{O}$ band at ~ 300 nm (Johnson 2000, Fig. 7), which is shortward of the feature identified here.

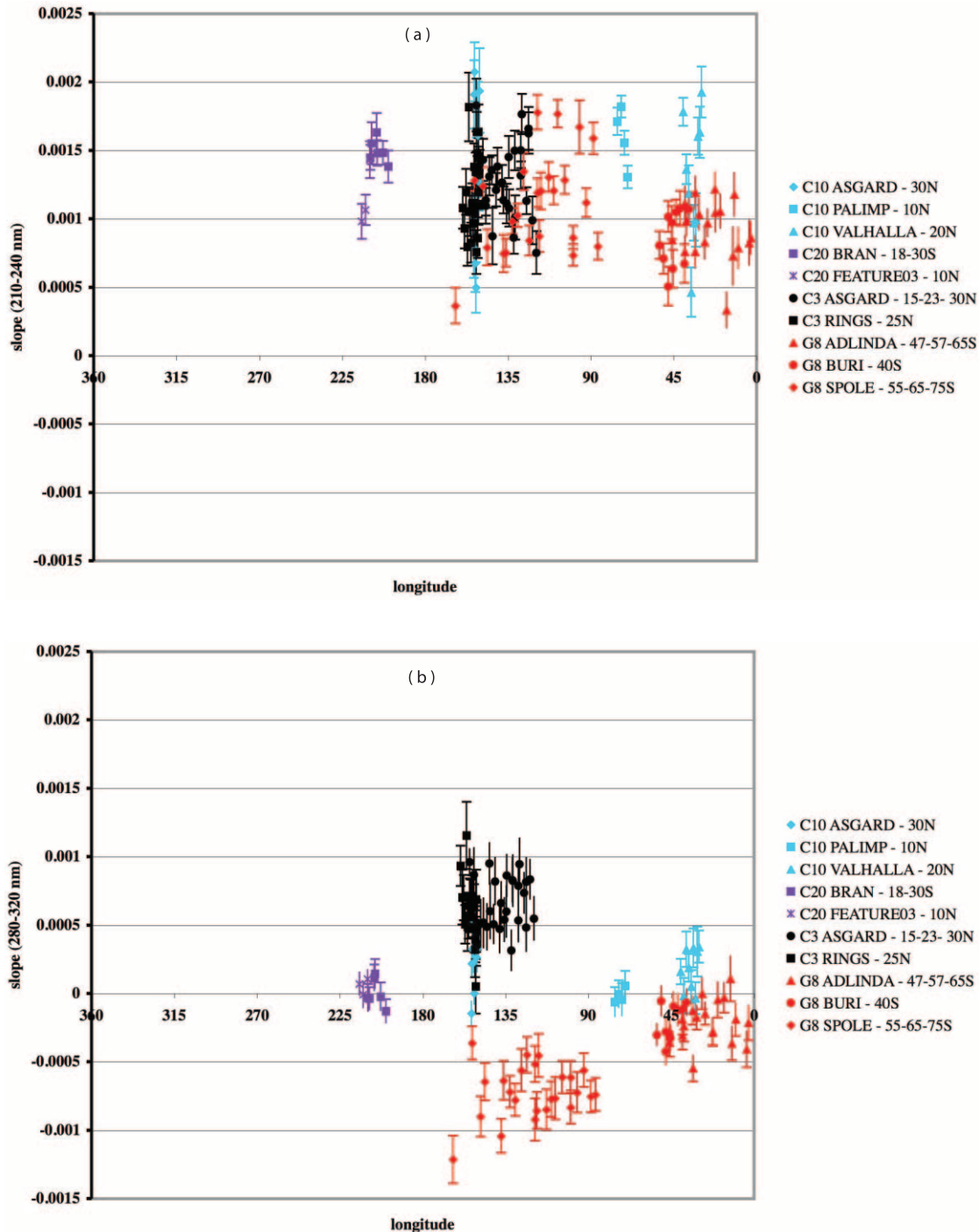


FIG. 4.—High-resolution observation spectral slopes for (a) 220–240 nm and (b) 280–320 nm vs. longitude. Slopes are in units of reflectance per Å. Error bars represent the 1σ uncertainty on the computed slopes.

The spectra in Figure 5 are normalized to each other at short wavelengths. Therefore, we also show spectra taken at similar phase angles to compare the absolute magnitude of the reflectance spectra: Figure 6 displays a high-latitude spectrum and a low-latitude (Asgard region) spectrum at similar solar phase angles. The low-latitude spectrum is darker than the high-latitude spectrum and, as previously stated, does not exhibit the long-wavelength feature.

One interpretation of the observed overall trend of the lower latitudes being generally darker and spectrally redder than the high-latitude regions is that an absorber (with band center >320 nm) is present at high latitudes, which is weathered or darkened by charged particle or UV irradiation at low latitudes. In addition,

there is a species present that is dark and red in the UV, possibly a result of weathering and chemical processing. Although the Asgard, Valhalla, and south pole region spectra, when normalized, lie on top of each other (Fig. 5), we see in the absolute spectra (Fig. 6) that the slopes are not the same: the low-latitude Asgard region clearly contains more of a reddish absorber. Based on Figure 5, this is likely the same material that gives the south pole region an overall red shape (at $\lambda < 280$ nm) as well. Spectra of candidate species that have been suggested are shown in Figure 7, including phyllosilicates. None of these species exhibits the long-wavelength absorption feature seen in the Callisto high-latitude spectra. We do find that spectra of several organics have

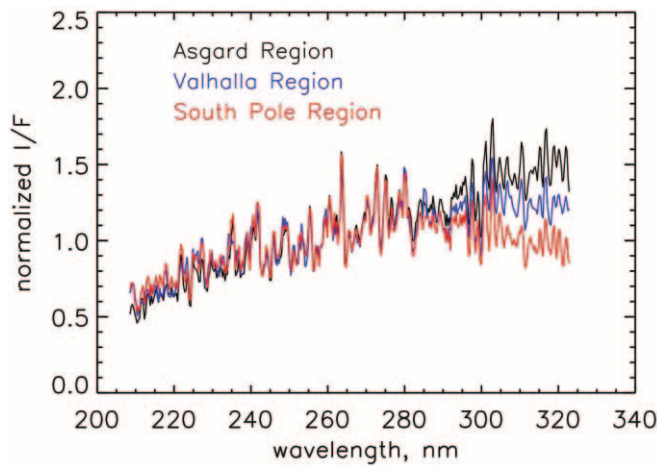


FIG. 5.—Sample reflectance spectra from different regions on Callisto. Spectra are scaled to unity at ~ 240 nm.

an absorption band near 350 nm, consistent with the apparent shoulder seen in the Callisto spectra. An example is shown in Figure 8.

4.3. Comparisons with Previous Results— Is there an SO_2 Feature?

An ultraviolet absorption feature centered near 280 nm appeared in disk-integrated *IUE* and *HST* of the leading hemisphere spectrum when it was ratioed to the trailing hemisphere spectrum (Lane & Domingue 1997; Noll et al. 1997) and was attributed to SO_2 . In the *IUE* reflectance spectra, the feature appeared more often in spectra from the “post-*Voyager*” (1984–1986) era than from the “*Galileo*” (1996) era; such a temporal change was attributed to changes in output of neutral sulfur from Io.

In the analysis of *HST* ratioed spectra by Noll et al. (1997), SO_2 was inferred by inspection of a ratio of the leading hemisphere spectrum (centered on 90° west) to the trailing hemisphere spectrum (centered on 280° west). It was suggested that either pre-existing Callisto sulfur is enhanced by micrometeoroid bombardment, or sulfur is brought in by micrometeoroids, the flux of which is enhanced on the leading hemisphere. However, below we question whether there really is a feature related to a sulfur species.

A broad 280 nm feature can also be produced in the *Galileo* UVS data (Fig. 3b) by ratioing low-resolution equatorial spectra

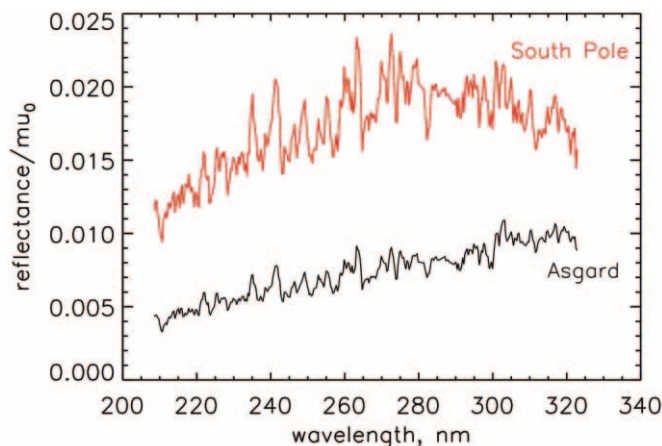


FIG. 6.—Reflectance spectra at similar phase angles (not normalized) from a high southern latitude region and from a low-latitude (Asgard) region. The low-latitude regions in general are darker than the high latitudes and do not exhibit the long-wavelength absorption band.

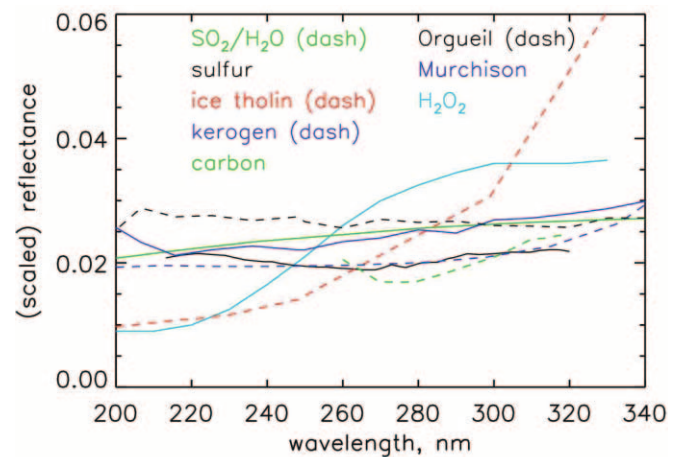


FIG. 7.—Reflectance spectra of candidate nonwater ice species.

from the leading hemisphere (77° – 135° west) to low-resolution equatorial spectra from the trailing hemisphere (longitudes 224° – 261° west) (Hendrix et al. 1998). However, *no such band* is seen in the absolute spectra in Figures 3a, 5, and 6. Therefore, we suggest that the identification of a UV band associated with a sulfur feature may have been induced when the spectra were ratioed and the interpretation was influenced by a similar identification at Europa. Considering that the atmosphere of Callisto is much thicker than that of Europa, the surface temperature is higher, allowing for enhanced redistribution of material, and the plasma flux is much smaller than at Europa, the lack of a sulfur feature due to transport of material from Io might not be surprising. However, we cannot rule out a small contribution, and some absolute (i.e., nonratioed) *IUE* spectra suggest a feature might be present (Lane & Domingue 1997).

Although a broad 280 nm feature can be produced by ratioing a leading hemisphere spectrum to a trailing hemisphere spectrum, it is questionable whether such a band is real. If SO_2 is present, then it might be observable in the IR. We note that spectral features attributed to sulfur dioxide were also suggested based on *Galileo* NIMS data (Hibbitts et al. 2000). That is, small bands appear in the NIMS spectra at ~ 3.88 and $\sim 4.05 \mu\text{m}$. However, Figure 20.11 of Johnson et al. (2004) shows that both NIMS features are more similar to carbonate features. Whereas the feature at $3.88 \mu\text{m}$ was initially suggested to be due to S-H stretch

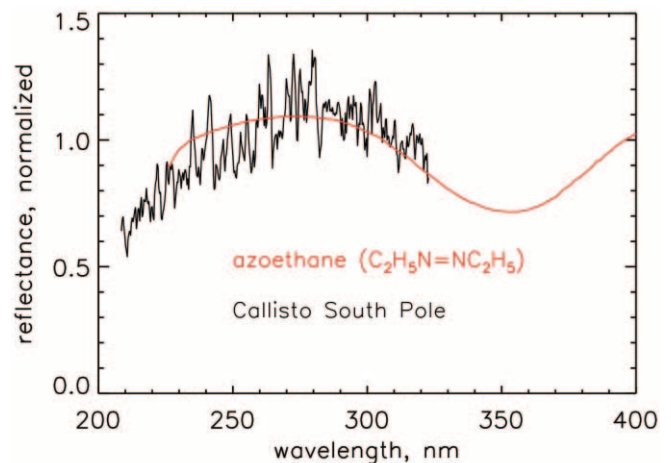


FIG. 8.—Sample organic species compared with the Callisto high-latitude absorption feature. Here the azoethane spectrum, measured as an absorbance in the laboratory, has been inverted to compare with the Callisto reflectance spectrum.

(McCord et al. 1997), it can better be associated with a material like carbonic acid (H_2CO_3 ; Johnson et al. 2004), which must be present if CO_2 in ice is exposed to radiation.

5. DISCUSSION AND CONCLUSIONS

A significant effect of ion bombardment of ices is the creation of new species through radiolysis. Bombarding particles can decompose H_2O ice, creating molecular hydrogen and oxygen. Whereas the hydrogen readily escapes to space, the O_2 does not; as a result, species such as O_3 , H_2O_2 , O_2 , and SO_2 have been detected as gases trapped in the regoliths of Europa and Ganymede. Ionizing radiation not only forms more complex molecules, it can efficiently decompose organics. At low doses, CO and CO_2 are the principal decomposition products of a number of organics and carbonates (e.g., Calvert & Pitts 1996). Callisto's CO_2 could be a decomposition product of an endogenic organic material (Johnson 2000) or of carbonaceous material delivered by meteorites. A carbon cycle may be occurring on Callisto, with CO_2 , carbonates and carbon suboxides as principal end-products (Johnson et al. 2004). The overall dark gray visible appearance of Callisto is consistent with laboratory measurements of carbonization of organics through radiation. Surfaces made up of organics exposed to high amounts of radiation (e.g., inner solar system, or older surfaces in the outer solar system) get darker and blacker (or grayer), whereas organic-containing surfaces exposed to less radiation are redder (Andronico et al. 1987). This explanation has been used, for instance, to explain the (visible) gray color of Phoebe compared to the red color of the dark material on Iapetus (Strazzulla 1986; Thompson et al. 1987; Allamandola et al. 1988; Owen et al. 2001) as well as the gray color of KBOs of large eccentricity with aphelions >70 AU compared to visibly redder, cold outer solar system KBOs (perihelion >40 AU; Tegler et al. 2003). We postulate here that the corresponding trend in the UV is toward older, more weathered regions on Callisto becoming darker and the 350 nm absorption band strength decreasing, which tends to give the spectrum an overall redder slope in the UV. An organic feature with an absorption band centered shortward of the feature seen here was suggested to account for the long-wavelength shoulder on the disk-averaged ozone absorption feature on Ganymede (Johnson 2000), although that needs to be confirmed by analysis of spatially resolved spectra now available.

Our *Galileo* UVS analysis has resulted in a possible detection of organics in the south polar region of Callisto. A plausible scenario is that organic species are present in the ice accounting in part for the red spectrum in the UV and the feature longward of 320 nm. These species are weathered away by UV and charged particle and micrometeoroid bombardment. The weathering processes, which are more prevalent at low latitudes than at high latitudes, result in carbonization of the organics, darkening of the ice, and decomposition of the organics to simple carbon chains. UV radiation, impervious to the atmosphere, will carbonize and darken the low latitudes at all longitudes, but the effect of the energetic plasma depends strongly on the thickness of the atmosphere. However, heavy corotating ions have been suggested as the source of the pattern in the adsorbed or trapped CO_2 pattern seen by NIMS (Hibbitts et al. 2002). The leading hemisphere has been suggested to be still slightly darker than the trailing hemisphere due to the enhanced delivery of organics by meteoroids (Buratti 1991).

Simple spectral models are consistent with the scenario described above involving weathered organics. For instance, we can model the high-latitude reflectance spectra with mixtures containing higher amounts of unprocessed organic material, while the lower latitude region spectra can be fit with mixtures of darker

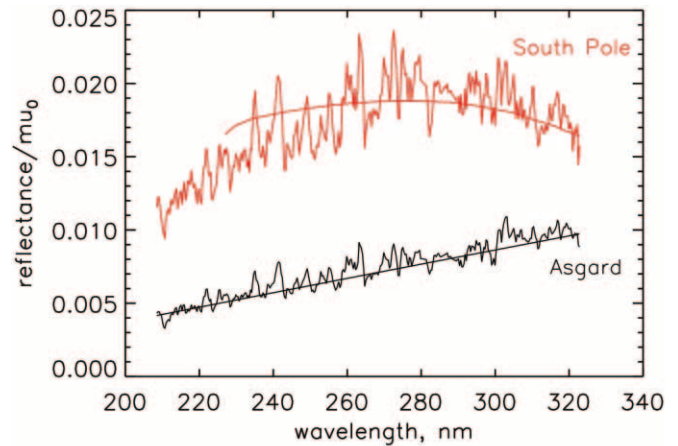


FIG. 9.—Sample models for comparison with Callisto spectra in Fig. 6. The low-latitude (Asgard) spectra can be modeled with carbon mixed with redder material, while the spectra of the higher latitudes can be explained largely by the presence of an unprocessed organic species such as azoethane (Fig. 8).

material, such as processed organic material as shown in Figure 9. In generating these simple models, we assumed a mixture of pure, unprocessed organic (azoethane) plus a small amount of water ice and a small amount of dark, spectrally red material for the high-latitude region; for the low-latitude region, we created a simple mixture of primarily dark, spectrally red material plus dark, spectrally neutral material (carbon). The dark, spectrally red material is assumed to represent processed organic material. Near-infrared measurements have also shown evidence for organic species on Callisto, possibly a CN compound, as indicated by a band at $4.57 \mu\text{m}$ (McCord et al. 1997). It is not clear whether this spectral feature appears more strongly at high latitudes, however.

Weathering of organics by radiolysis and meteoroid-induced mixing may account for the differences between hemispheres and the spectral variations reported here, but alternate scenarios are possible. Carbon dioxide could be the result of outgassing from primordial materials that are preferentially more stable at the poles. There the rate of photolytic processing would be smaller than the equator, producing simple organics that have a band minimum above ~ 320 nm, whereas species are preferentially carbonized at lower latitudes.

The spectrally flat shape at $\lambda > 280$ nm, seen in some regions across Callisto, is not unlike the spectral characteristic of H_2O_2 , and appears largely on the trailing hemisphere (Fig. 3a) and in isolated regions of the leading hemisphere (e.g., the Valhalla regions spectrum in Fig. 5). If the feature is due to peroxide, we expect that it would be the result of radiolytic processing of local concentrations of H_2O ice; Callisto's surface ice fraction is 20%–45% (Calvin et al. 1995). In an earlier analysis (Hendrix et al. 1999), the maximum concentration of hydrogen peroxide on Callisto was estimated to be $\sim 0.1\%$, compared with a maximum concentration on Europa of $\sim 0.24\%$. This could be a low enough concentration that the $3.5 \mu\text{m}$ H_2O_2 feature would not be present in NIMS data sets. Alternately, the spectral shape could be due to relatively small amounts of the organic species that appears in larger concentrations at high latitudes, causing the long-wavelength rollover. Peroxide could be partly responsible for the reddish slope of the Callisto UV spectra, although we suggest that carbon-based species in varying amounts dominate the reddening of the spectral slope.

In summary, low-resolution observations have been analyzed to look for global spectral trends across the surface. No major spectral variations are found with the following exceptions: the

leading hemisphere is slightly redder than the trailing hemisphere, at $\lambda > 280$ nm, while the trailing hemisphere is largely spectrally flat at $\lambda > 280$ nm. Analysis of *IUE* and *HST* observations (Noll et al. 1997; Lane & Domingue 1997) ratioed disk-averaged spectra producing a band thought to correspond to SO₂ on the leading hemisphere. Although small amounts of SO₂ could be present, here we suggest that a feature that appears to be a band could be produced when spectra are ratioed, as seen in Figure 3*b*.

The high spatial resolution observations presented here suggest the presence of an absorption band with a band minimum ≥ 320 nm that is strongest at high latitudes. Here we suggest that this feature is due to an organic species that is weathered (carbonized and darkened) at lower latitudes and that the overall darker leading hemisphere is due to emplacement of material by impacting meteoroids. Certainly the composition of Callisto's surface is spatially variable and the situation is not as simple as

the low latitudes having a uniform spectra due to weathering (e.g., Fig. 5). Further analysis of this interesting data combined with reanalysis of the earlier *IUE* and *HST* results may indicate whether the carbon-containing species suggested to be present have as their ultimate source endogenic or implanted organics or are produced following outgassing of carbon dioxide.

The authors acknowledge support from NASA's Planetary Geology and Geophysics Program and thank Anne Verbiscer for helpful comments on the manuscript. A. R. H. thanks Karen Simmons for assistance with *Galileo* UVS data. This work was performed at the Jet Propulsion Laboratory, California Institute of Technology, under contract with the National Aeronautics and Space Administration.

REFERENCES

- Allamandola, L. J., Sandford, S. A., & Valero, G. J. 1988, *Icarus*, 76, 225
 Andronico, G., Baratta, G. A., Spinella, F., & Strazzullam, G. 1987, *A&A*, 184, 333
 Buratti, B. J. 1991, *Icarus*, 92, 312
 Calvin, W. M., & Clark, R. N. 1991, *Icarus*, 89, 305
 ———. 1993, *Icarus*, 104, 69
 Calvert, J. G., & J. Pitts 1996, *Photochemistry* (New York: Wiley)
 Calvin, W. M., Clark, R. N., Brown, R. H., & Spencer, J. R. 1995, *J. Geophys. Res.*, 100, 19041
 Carlson, R. W. 1999, *Science*, 283, 820
 Cooper, J. F., Johnson, R. E., Mauk, B. H., Garrett, H. B., & Gehrels, N. 2001, *Icarus*, 149, 133
 Hendrix, A. R. 1996, Ph.D. thesis, Univ. Colorado
 Hendrix, A. R., Barth, C. A., Hord, C. W., Lane, A. L., Tobiska, W. K., & Simmons, K. E. 1998, in *Proc. 29th Lunar and Planetary Sci. Conf.* (Houston: LPI), 1865
 Hendrix, A. R., Barth, C. A., Stewart, A. I. F., Hord, C. W., & Lane, A. L. 1999, in *Proc. 30th Lunar and Planetary Sci. Conf.* (Houston: LPI), 2043
 Hendrix, A. R., Domingue, D. L., & King, K. 2005, *Icarus*, 173, 29
 Hibbitts, C. A., McCord, T. B., & Hansen, G. B. 2000, *J. Geophys. Res.*, 105, 22541
 Hibbitts, C. A., Klemaszewski, J. E., McCord, T. B., Hansen, G. B., & Greeley, R. 2002, *J. Geophys. Res.*, 107(E10), 5084, doi:10.1029/2000JE001412
 Hord, C. W., et al. 1992, *Space Sci. Rev.*, 60, 503
 Johnson, R. E. 2000, in *Chemical Dynamics in Extreme Environments*, ed. R. A. Dressler (Singapore: World Scientific), 390
 Johnson, R. E., Carlson, R. W., Cooper, J. F., Paranicas, C., Moore, M. H., & Wong, M. C. 2004, in *Jupiter: The Planet, Satellites and Magnetosphere*, ed. F. Bagenal, T. E. Dowling, & W. B. McKinnon (Cambridge: Cambridge Univ. Press), 485
 Kliore, A. J., Anabtawi, A., Herrera, R. G., Asmar, S. W., Nagy, A. F., Hinson, D. P., & Flasar, F. M. 2002, *J. Geophys. Res.*, 107, 1407, DOI: 10.1029/2002JA009365
 Lane, A. L., & Domingue, D. L. 1997, *Geophys. Res. Lett.*, 24, 1143
 Lane, A. L., Nelson, R. M., & Matson, D. L. 1981, *Nature*, 292, 38
 Liang, M.-C., Lane, B. F., Pappalardo, R. T., Allen, M., & Yung, Y. L. 2005, *J. Geophys. Res.*, 110, E02003, DOI: 10.1029/2004JE002322
 McCord, T. B., et al. 1997, *Science*, 278, 271
 Moore, J. M., et al. 2004, in *Jupiter: The Planet, Satellites, and Magnetosphere*, ed. F. Bagenal, T. E. Dowling, & W. B. McKinnon (Cambridge: Cambridge Univ. Press), 397
 Nelson, R. M., Lane, A. L., Matson, D. L., Veeder, G. J., Buratti, B. J., & Tedesco, E. F. 1987, *Icarus*, 72, 358
 Noll, K. S., Johnson, R. E., McGrath, M. A., & Caldwell, J. J. 1997, *Geophys. Res. Lett.*, 24, 1139
 Owen, T. C., et al. 2001, *Icarus*, 149, 160
 Pilcher, C. B., Ridgway, S. T., & McCord, T. B. 1972, *Science*, 178, 1087
 Rottman, G. J., Woods, T. N., & Sparr, T. P. 1993, *J. Geophys. Res.*, 98, 10667
 Roush, T. L., Pollack, J. B., Witteborn, F. C., Bregman, J. D., & Simpson, J. P. 1990, *Icarus*, 86, 355
 Spencer, J. R., & Calvin, W. M. 2002, *AJ*, 124, 3400
 Stebbins, J., & Jacobsen, T. S. 1928, *Lick Obs. Bull.*, 13, 180
 Strobel, D. F., Saur, J., Feldman, P. D., & McGrath, M. A. 2002, *ApJ*, 581, L51
 Strazzulla, G. 1986, *Icarus*, 66, 397
 Tegler, S. C., Romanishin, W., & Consolmagno, G. J. S. J. 2003, *ApJ*, 599, L49
 Thompson, W. R., Murray, B. G. J. P. T., Khare, B. N., & Sagan, C. 1987, *J. Geophys. Res.*, 92, 14933